EFFECT OF GTAW ON THE TENSILE STRENGTH AND HARDNESS OF MILD STEEL

S. Elfallah*

Mechanical Engineering Department, College of Mechanical Engineering Technology, Benghazi, Libya
*Corresponding author's e-mail address: sselfallah87@gmail.com

ABSTRACT

Gas tungsten metal arc welding (GTAW) is used to study the effect of the base metal thickness, welding current and welding speed on the tensile strength and hardness of mild steel welding. The analysis found that base metal thickness had the highest effect and highest means of tensile strength and hardness of the welding. Taguchi's design (TD) suggested using higher base metal thickness, lower welding current and higher welding speed when welding mild steel in order to obtain maximum tensile strength and hardness. The welding that has higher tensile strength showed higher hardness. However, the hardness increased proportionally with the increased internal stresses of the welding. The welding showed wider heat affected zone (HAZ) with the increase in internal stresses of the welding.

1. INTRODUCTION

GTAW is a welding technology that is considered a vital process, as it has multiple goals and factors in the industrial sector [1]. It is also advantageous in dissimilar welding and produces minimum HAZ with no slag and narrower bead geometry [2]-[4]. GTAW uses non-consumable tungsten electrode and shield gas (e.g., argon or helium) to protect the weld pool from air contamination [2], [4]. The quality of GTAW depends on finding out the optimum practical welding condition. Such optimization should satisfy the desired welding objectives [5]. The welding quality depends on the welding process factors, which will lead to certain chemical, mineral and mechanical properties of the welding [6], [7]. By controlling the welding factors, the mechanical properties of welding are controllable. The interaction of multiple process factors in a complex manner leads to direct or indirect effects on the mechanical properties of the welding [1].

Taguchi's design (TD) is a technique devised by Dr. Genichi Taguchi. A partial factorial method of experimental design called an orthogonal array that requires much less trials than the traditional full factorial design of experiments [8]. TD will be used to optimize the process of experimentation in an effort to improve welding productivity and quality. TD is considered simple, and it is increasingly used in manufacturing industries [9].

Ramadan and Boghdadi [1] studied the effect of welding gas flow rate and welding current on the tensile strength of low carbon steel dissimilar joint using TD. Anand, Mittal and Scholar [10] showed the effect of welding voltage, welding current and welding gas flow rate on the tensile strength and hardness of mild steel dissimilar joint using TD. They found that the welding current had a higher effect on the tensile and hardness of the welding.

Researchers reported that the welding that has high tensile strength also has higher hardness [10], [11]. However, Talabi et al. [12] concluded that the welding that has higher tensile strength has lower hardness. In general, both the tensile strength and hardness of the welding decrease with the increase of the welding voltage and current [13,14]. Because of the increase, it increases the heat input in the weld pool, causing internal stresses in the fusion zone (FZ) and HAZ and consequently the welding's mechanical properties' deterioration such as tensile strength and hardness while the toughness increases [11]. From microstructure prospective, the cause of low tensile strength and hardness is due to the coarse and dendritic grain structure in FZ [11]. However, Sankar et al. [15] have reported that FZ and HAZ have higher hardness than the base metal because of the ferrite with the pearlite presence in the structure.

This study will investigate and optimize the effect of GTAW current, base metal thickness and welding speed on mild steel in order to find the factors leading to the optimum tensile strength and hardness for better performance and higher quality welding. The analysis for TD will be made using Minitab 18®. Also, microstructure analysis will be carried out in order to see the behaviour of the welding structure

besides the mechanical testing of tensile and hardness of the welding.

2. MATERIALS AND METHODS

Mild steel was purchased from the local market and was prepared in Tasamim workshop, in Benghazi, using a CNC laser cutter. The preparation of the samples was made according to the American society of testing materials (ASTM) E8 / E8M for the tensile test [16]. Figure 1 shows an illustration of the sample with the dimensions for the tensile test with a V groove of 60°. Also, other samples were prepared for hardness testing in the same workshop. The welding of the samples took place at Altaibat Food Inc, in

Benghazi. The welding was achieved by Daewoo Inverter Welder TIG/MMA with the aid of the welding speed machine YSG-12 Beetle Portable Gas Cutter. The tungsten electrode tip was kept 3 mm away from the base metal (Fig. 2). The welding process is shown in figure 3. The shielding gas used is composed of 90% argon and 10% carbon dioxide with a flow of 10 millilitres per minute. The voltage is estimated to be between 20 and 30 V. Table 1 lists the composition of the base metal and filler wire. The base metal is non-alloy structural steel European standard EN 10025-2, grade S235JR (1.0038), and the welding filler used is E6013 (2.5 mm in diameter) mild steel. Table 2 shows the tensile strength and hardness properties of the base metal and filler wire.

Table 1. The chemical compositions of the base metal and welding wire used in the experiment [17]

Component	Chemical Composition									
	C	Mn	S	Ni	Cr	P	Si	Cu	Mo	V
Base metal (EN 10025-2)	0.17%	1.4%	0.025%	0.012%	-	0.025%	-	0.55%	-	-
Welding filler (E6013)	0.10%	0.6%	0.03%	0.3%	0.2%	0.035%	0.5%	0.35%	0.2%	0.05%

Table 2. The tensile strength and hardness of base metal and filler wire [18], [19]

Component	Tensile properties			Hardness	
	Yield strength	Tensile strength	Elongation	Brinell hardness	Vickers micro-hardness
Base metal	235	360-510	26%	≤120 HBW	≈2025 HV
Welding filler	483 MPa (70 ksi)	583 MPa (81 ksi)	26%	-	-
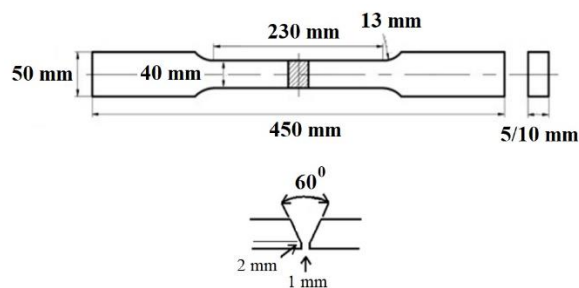
Fig. 1. Samples dimensions for tensile test made according to ASTM E8/E8M [16]
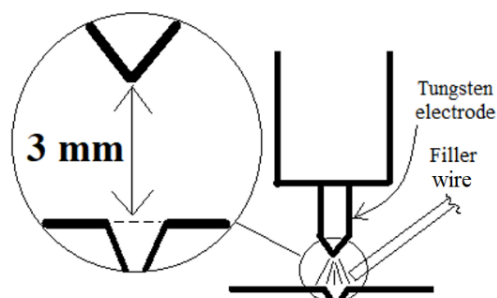
Fig. 2. Tungsten tip position with respect to the base metal

Fig. 3. Welding process

The welding factors are base metal thickness, welding current and welding speed that are used for the welding process. Each has two levels as listed in table 3, which according to TD results in 4 runs. However, with such low numbers of runs the coefficient and ANOVA analysis could not be generated. Therefore, TD allows 8 runs (L8 array) in order to perform the analysis. Table 4 shows TD coding layout concerning the welding parameters levels. The analysis was made using the Minitab 18®.

Table 3. Main process parameters

Code	Factors	Unit	Level 1	Level 2
A	Base metal thickness	cm	5	10
B	Welding current	A	150	200
C	Welding speed	mm/min	100	150

Table 4. Coded design layout values

Standard order	A	B	C
1	1	1	1
2	1	1	2
3	1	2	1
4	1	2	2
5	2	1	1
6	2	1	2
7	2	2	1
8	2	2	2

Tensile test carried out on Shimadzu (UEH-20) universal testing machine at Libyan Iron and Steel Company at Misrata. The tested samples are shown in figure 4. Some of these samples were repeated due to the failure of the first ones. The hardness test was conducted in the High Vocational Center of Casting at Tripoli with a BMS Bulut Makina Sanayi Vickers micro-hardness tester.

The indenter was a diamond cone with a load of 1 kg as pressure force. The microstructure of the welding was obtained using a Zeiss Axio Cam optical microscope. The hardness and microstructure were examined for the FZ and HAZ. An average of three readings was recorded for the FZ and HAZ.

Table 4 shows the TD layout according to welding factors and their corresponding tensile strength and Vickers micro-hardness of the welding.

Fig. 4. Samples used for tensile strength

Table 5. Tensile strength and Vickers micro-hardness results versus process parameters

Sample No.	Base metal thickness [mm]	Welding current [A]	Welding speed [mm/min]	Tensile strength [MPa]	Heat input [J/mm]	Vickers micro-hardness [HV] FZ	Vickers micro-hardness [HV] HAZ	[MPa] / HV
1	5	150	100	183	2700.0	2093	2104	0.087
2	5	150	150	190	1800.0	2121	2087	0.090
3	5	200	100	159	3600.0	1897	2091	0.084
4	5	200	150	171	2400.0	1948	2043	0.088
5	10	150	100	304	2700.0	3439	3570	0.088
6	10	150	150	270	1800.0	2794	2846	0.097
7	10	200	100	237	3600.0	2678	2775	0.088
8	10	200	150	251	2400.0	2686	2750	0.093

3. RESULTS AND DISCUSSIONS

The results in table 5 showed that the hardness increased whenever the tensile increased and vice versa. The hardness for the HAZ is higher than that of the FZ. Also, higher tensile strength and hardness were obtained with the increase in base metal thickness and welding speed, except for sample no.5 when compared with sample no.6, while the current decreased. The higher current and slower welding resulted in higher heat input as seen in table 5. The main factor that affected the decreased tensile strength was the welding current at fixed base metal thickness. The prolonged heat in the welding leads to higher dilution of the fusion zone, which means wider weld bead and therefore to increased internal stresses [3], [11]. Higher internal stresses cause lower mechanical properties such as lower tensile strength while the hardness increases according to Talabi et al. [12]. The tensile strength has decreased with higher heat input, however, not for all cases. Where the tensile increased for sample no.1 compared to 4, and 4 compared to 8 when assuming fixed base metal thickness. Interestingly the tensile strength to hardness ratio as presented in table 5 showed lower ratio at higher heat input. This means proportionally higher ratio compared to the given tensile strength. The lower base metal thickness causes a lower cooling rate with the welding surrounding because of the less amount of surrounding metal compared to the thicker joints as it can act as a heat sink to the welding. So, the welding with higher joint thickness

solidifies faster than welds of lower joint thickness.

Jeet et al. [20] have explained that the increased tensile strength and hardness correspond to increase in thickness of the base metal. Higher base metal thickness means more surrounding area around the fusion zone of the welding area. This area acts as a heat sink that absorbs heat from the weldment and distributes it to the base metal. Yadav et al. [21] showed that base metal thickness increase has contributed to increased tensile strength and hardness of the HAZ.

The following plots (Fig. 5) and (Fig. 6) are the effects plots for signal-to-noise (S/N) ratios and the means of the welding factors.
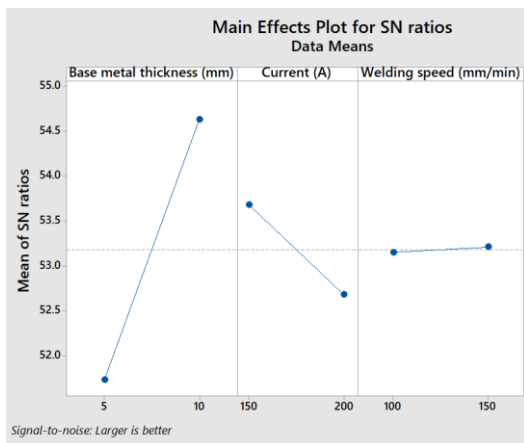
Fig. 5. S/N ratio plot for the welding factors
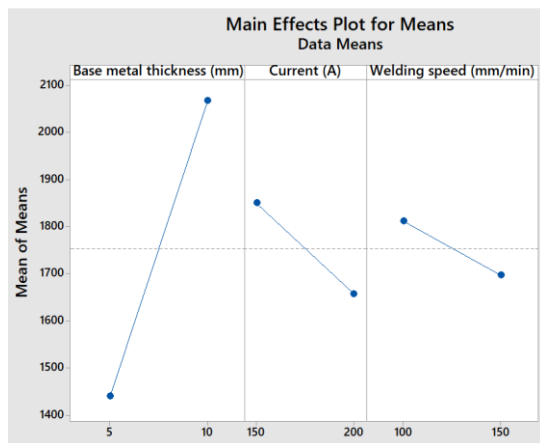
Fig. 6. Means plot for the welding factors

The two plots show similar orientation of results to a high extend. The S/N ratios in figure 5 show the welding factors' S/N ratios in relation to the S/N mean. The S/N ratio measures the effect or influence of the welding factors on the higher tensile strength and hardness values by showing how each welding factor level varies with respect to the response (higher tensile strength and hardness) under different noise conditions. The higher S/N ratio is labelled in figure 5 and table 6 as "Larger is Better", which corresponds to the experiment goal, that is to maximize the

response. The values of each S/N ratio are shown in table 6 at each level, while the Delta is a result of the higher S/N ratio minus the lower. The ranking is based on the higher Delta value, which indicates the strength of each welding factor for each level. It is also indicated by the absolute values of the coefficient for S/N ratios in table 7. However, the coefficient values are only for Level 1 welding factors. The most influencing level on the higher results is 10 mm base metal thickness followed by 150 A and 150 mm/min. While the base metal thickness at 5 mm had the lowest effect on the higher response. The means plot in figure 6 shows the response means in relation to the average of means. Table 7 shows the averages at each level of welding factor, delta and ranking based on response means. It is shown in figure 6 and table 7 that the base metal at 10 has the highest response mean or average followed by a welding current of 150 A and welding speed of 100 mm/min. The base metal of 5 mm has the lowest response mean.

Table 6. Response ranking for S/N ratios

Level	Base metal thickness (mm)	Welding current (A)	Welding speed (mm/min)
1	51.73	53.68	53.15
2	54.62	52.68	53.20
Delta	2.90	1.00	0.06
Rank	1	2	3

*Larger is better

Table 7. Response ranking for Means

Level	Base metal thickness [mm]	Welding current [A]	Welding speed [mm/min]
1	1441	1850	1811
2	2067	1657	1696
Delta	626	193	115
Rank	1	2	3

Table 8. Coefficients for S/N ratios

Term	Coefficient	P-value
Constant	53.1759	0.000
Base metal thickness (5 mm)	-1.4486	0.001
Welding current (150 A)	0.5000	0.027
Welding speed (100 mm/min)	-0.0287	0.854

Table 9. Coefficients for Means

Term	Coefficient	P-value
Constant	1753.71	0.000
Base metal thickness (5 mm)	-313.12	0.006
Welding current (150 A)	96.54	0.175
Welding speed (100 mm/min)	57.29	0.384

Table 8 and table 9 show the S/N ratios and means coefficients estimated model for welding factors. Table 7 shows the smallest P-value (population value) for a thickness of 5 mm at 0.001. Which is lower than the significance value of 0.05 (95%) and therefore is considered significant. In other words, the effect of base metal thickness at 5 mm has a 99.9% occurrence rate of repetition and thus rejects the null hypothesis. The welding current of 150 A has also shown to be significant with a 97.3 % rate of occurrence. However, the welding speed of 100 mm/min did not obtain significance with only a 14.6 % occurrence rate. The base metal thickness at 5 mm has also shown a significant rate of repetition with 99.4 %, while the welding current at 150 A obtained a non-significant rate of 82.5 %. The welding speed at 100 mm/min has a lower percentage of occurrences with only 61.6%. It indicates that if the experiment is repeated there is a chance of 61.6% that the welding speed of 100 mm/min will present similar results. Minitab 18[®] did not show P-values for level 2 factors.

Figure 7 shows the microstructure magnified 100 times of the base metal of 10 mm thickness, where the microstructure shows the ferrite (α) and perlite (P) grains. The ferrite has a fine round grain structure with light contrast that is mainly iron, while the perlite has coarse dark grains that have mainly iron carbide. The mild steel has 0.17% carbon content, which justifies the lesser perlite grains compared to ferrite.
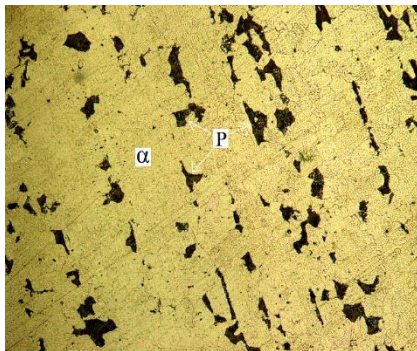
Fig. 7. Base metal microstructure of mild steel magnified at 100X
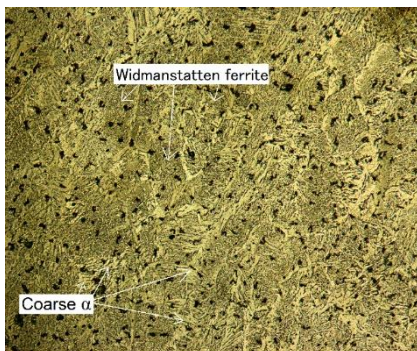
Fig. 8. FZ microstructure of welding conducted at 200 A and 100 mm/min magnified at 100X

Fig. 9. FZ microstructure of welding conducted at 200 A and 150 mm/min magnified at 100X
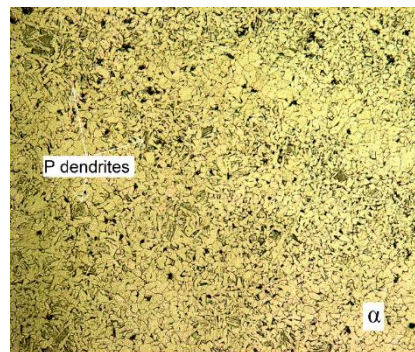
Fig. 10. HAZ microstructure of welding conducted at 200 A and 100 mm/min magnified at 100X
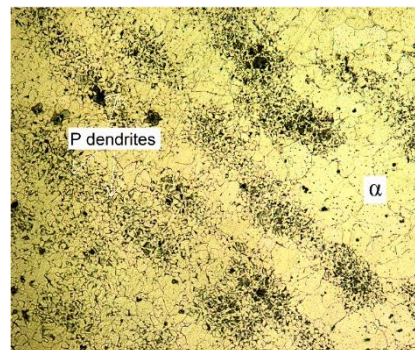
Fig. 11. HAZ microstructure of welding conducted at 200 A and 150 mm/min magnified at 100X

Figure 8 and figure 9 show the fusion zone microstructure for welding conducted at welding speeds of 150 mm/min and 100 mm/min. They correspond to samples no. 7 and no. 8 in the order listed in Table 5. The dark round holes are the porosity that resulted from welding. Both examples were welded at 200 A.

Both figures showed spread of the Widmanstatten ferrite under the form of sharp spiny ferrite grains scattered with coarse ferrite. While the perlite showed minute longitudinal grains exist between the ferrite grains. These grains are a result of the turbulence created in the weld pool and affected by the solidification process. While it is not the case for the

base metal (Fig. 7), which has gone through heat treatment processes that resulted in larger and round fine grains with clear precipitation of perlite, it is also clear that Widmanstatten ferrite is present in much larger areas than coarse ferrite structures when the welding speed is higher (Fig. 8 and Fig. 9). This is also clear in the HAZ structure as shown in figures 10 and 11, where a larger perlite dendrites structure is shown at a higher welding speed with respect to ferrite. The ferrite has shown finer grains at HAZ due to the recrystallization processes at slower welding speed as illustrated in figure 10 compared to figure 11. It is also an indication that a larger HAZ area has resulted in a slower welding speed (Fig. 10).

It is noticed that the welding that showed larger areas of Widmanstatten ferrite in the FZ and wider areas of perlite dendrites at HAZ has shown lower tensile strength with higher proportional hardness as presented in sample no. 7 in Table 5. This resulted from the slower welding speed that caused higher internal stresses as mentioned earlier. Therefore, it is clearly indicated that higher heat input caused a wider HAZ area that resulted in lower tensile strength with an increase in the hardness of welding.

4. CONCLUSIONS

GTAW is used to weld mild steel using factors of base metal thickness, welding current and welding speed. TD was made to analyze the effect of these factors on the maximized tensile strength and hardness of the welding. The results demonstrated that base metal thickness affected the higher result the most and also showed higher results means followed by welding current while the welding speed had a lower influence and means on the results. According to TD, it is recommended to use higher base metal thickness, lower welding current and higher welding speed to weld mild steel using GTAW. The welding that has higher tensile strength has higher hardness. However, the increased heat input that resulted from increased welding current and the slower welding speed showed lower tensile strength and proportionally higher hardness. Higher base metal thickness showed higher tensile strength and proportionally lower hardness due to the heat sink phenomena. This disperses the heat input faster and lowers the resulting internal stresses in the welding. According to the welding microstructure, higher heat input due to slower welding results in wider areas of Widmanstatten ferrite in the FZ and wider HAZ, which indicates higher internal stresses.

ACKNOWLEDGEMENTS

REFERENCES

[1]. **Greyjevo O. G. T. V. Z., Metodo A. I. T.,** *Optimization of weld bead geometry in TIG welding process using grey relation analysis and Taguchi method,* Materiali in Tehnologije, vol. 43, iss. 3, 2009, pp. 143–149.

[2]. **Anand, K. R., Mittal, V., Scholar, P. G.** *Parameteric optimization of TIG welding on joint of stainless steel (316) & mild steel using taguchi technique,* International Research Journal of Engineering and Technology, 2017, pp. 366–370.

[3]. **Vikesh Randhawa J., Suri N. M.,** *Effect of A-TIG welding process parameters on penetration in mild steel plates,* International Journal of Mechanical and Industrial Engineering, vol. 4, iss. 1, 2014, pp.76-79.

[4]. **Cary H. B., Helzer S.,** *Modern welding technology,* 6rd ed., Pearson: US, 2004.

[5]. **Ramadan N., Boghdadi A.,** *Parametric optimization of TIG welding influence on tensile strength of dissimilar metals SS-304 and low carbon steel by using Taguchi approach,* American Journal of Engineering Research, vol. 9, no. 9, 2020, pp. 7–14.

[6]. **Pasupathy J., Ravisankar V.,** *Parametric optimization of TIG welding parameters using Taguchi method for dissimilar joint (Low carbon steel with AA1050).* Journal of Scientific & Engineering Research, vol. 4, 2013, pp. 25-28.

[7]. **Srirangan A. K., Paulraj S.,** Multi-response optimization of process parameters for TIG welding of Incoloy 800HT by Taguchi grey relational analysis, Engineering Science and Technology, an International Journal, vol. 19, no. 2, 2016, pp. 811-817.

[8]. **Taguchi G., Jugulu, R., Taguchi S.,** *Computer-based Robust Engineering: Essentials for DFSS,* ASQ Quality Press, Wisconsin, USA, 2004.

[9]. **Tanco M., Viles E., Ilzarbe, L., Álvarez M. J.,** *Manufacturing industries need design of experiments (DoE),* World Congress on Engineering, vol. 20, 2007, pp. 1108–1113.

[10]. **Ragh R., Somasundaram, S.,** *An optimization of welding parameters for MIG welding,* Int. Journal of Engineering Research and Technology, vol. 6, iss.14, 2018, pp.1-5.

[11]. **Bodude, M. A., Momohjimoh, I.** *Studies on effects of welding parameters on the mechanical properties of welded low-carbon steel,* Journal of Minerals and Materials Characterization and Engineering, vol 3, iss. 3, 2015, pp. 142–153.

[12]. **Talabi S. I, Owolabi O. B., Adebisi J. A., Yahaya T.,** *Effect of welding variables on mechanical properties of low carbon steel welded joint,* Advanced Production Engineering Management, vol.9, iss.4, 2014, pp.181-186.

[13]. **Elfallah S. S. S.,** *Influence of GMAW parameters on the tensile strength of commercial steel,* International Science and Technology Journal, vol.29, 2022, pp.1-16.

[14]. **Elfallah S. S.,** *Effect of GMAW on the tensile strength and hardness of commercial steel,* International Journal of Computer Sciences and Engineering, vol. 10, no. 9, 2022, pp. 14-20.

[15]. **Sankar N., Malarvizhi S., Balasubramanian. V.,** *Mechanical properties and microstructural characteristics of rotating arc-gas metal arc welded carbon steel joints,* Journal of Mechanical Behaviour of Materials, vol.30, iss.1, 2021, pp.49-58.

[16]. ***** **American Society for Testing and Materials,** *Standard test methods for tension testing of metallic materials,* ASTM International, 2021.

[17]. ***** **World Material,** *EN 1.0038 steel S235JR material equivalent, properties, composition,* 2022, https://www.theworldmaterial.com/1-0038-steel-s235jr-material/

[18]. **Ratiwi Y. R., Wibowo S. S.,** *The Effect of Electrode and Number of Passes on Hardness and Micro Structure of Shielded Metal Arc Welding,* In IOP Conference Series: Materials Science and Engineering. IOP Publishing, vol. 515, iss. 1, 2019, pp. 012072.

[19]. ***** **Wilson,** Hardness conversion table (DIN EN ISO 18265), 2020.

[20]. **Jeet S., Barua A., Parida B., Sahoo B. B., Bagal D. K.,** *Multi-objective Optimization of Welding Parameters in GMAW for Stainless Steel and Low Carbon Steel Using Hybrid RSM-TOPSIS-GA-SA Approach,* International Journal of Technical Innovation in Modern Engineering & Science, vol. 4, 2018, pp. 683–692.

[21]. **Yadav P. K., Abbas M., Patel S.,** *Analysis of heat affected zone of mild steel specimen developed due to MIG welding,* International Journal of Mechanical Engineering and Robotics Research, vol. 3, no. 3, 2014, pp. 399–404.